Article:

Qian, C. orcid.org/0000-0001-6158-9494, Ye, Y., Jiang, J. et al. (6 more authors) (2024) Rapid attribution of the record-breaking heatwave event in North China in June 2023 and future risks. Environmental Research Letters, 19 (1). 014028. ISSN 1748-9326

https://doi.org/10.1088/1748-9326/ad0dd9

ENVIRONMENTAL RESEARCH
LETTERS

LETTER • OPEN ACCESS

Rapid attribution of the record-breaking heatwave event in North China in June 2023 and future risks

To cite this article: Cheng Qian *et al* 2024 *Environ. Res. Lett.* **19** 014028

ENVIRONMENTAL RESEARCH
LETTERS

CrossMark

OPEN ACCESS

RECEIVED
1 August 2023

REVISED
13 October 2023

ACCEPTED FOR PUBLICATION
17 November 2023

PUBLISHED
7 December 2023

LETTER

Rapid attribution of the record-breaking heatwave event in North China in June 2023 and future risks

Cheng Qian[1,2,*], **Yangbo Ye**[1,2], **Jiacheng Jiang**[1,2], **Yangyang Zhong**[1,2], **Yuting Zhang**[1,2], **Izidine Pinto**[3], **Cunrui Huang**[4,5], **Sihan Li**[6] **and Ke Wei**[7]

[1] Key Laboratory of Regional Climate–Environment for Temperate East Asia, Institute of Atmospheric Physics, Chinese Academy of Sciences, Beijing, People's Republic of China
[2] University of Chinese Academy of Science, Beijing, People's Republic of China
[3] Royal Netherlands Meteorological Institute (KNMI), De Bilt, The Netherlands
[4] Institute of Healthy China, Tsinghua University, Beijing, People's Republic of China
[5] Vanke School of Public Health, Tsinghua University, Beijing, People's Republic of China
[6] Department of Geography, University of Sheffield, Sheffield, United Kingdom
[7] Center for Monsoon System Research, Institute of Atmospheric Physics, Chinese Academy of Sciences, Beijing, People's Republic of China
[*] Author to whom any correspondence should be addressed.

E-mail: qianch@tea.ac.cn

Keywords: heatwaves, event attribution, anthropogenic climate change, human influences, empirical approach, coupled model approach

Supplementary material for this article is available online

Abstract

A record-breaking heatwave event occurred in North China from 22 to 24 June 2023, with temperatures >40 °C at many meteorological stations. This marked the first time that Beijing had reached or exceeded 40 °C for three consecutive days. However, the extent to which such exceptional heatwave events are related to anthropogenic climate change remains unclear. It is also unclear how frequent and intense such strong heatwave events will be in the future. We carried out a rapid attribution analysis to address these questions. Our findings show that the return period of this three-day heatwave event in North China is about 111 years (24.3, $+\infty$) at the 2023 climate state. Both the empirical and coupled model approaches consistently showed that the intensity of 2023-like three-day heatwave events has significantly increased by at least 1.0 °C (range 0.8 °C–1.3 °C) due to anthropogenic climate change. Future projections indicate that 2023-like events in North China are likely to occur at least 1.6 (range 1.3–2.1) times throughout the remainder of this century and be 0.5 °C (range 0.2 °C–0.8 °C) more intense than those under the 2023 climate even if carbon neutrality is achieved based on the very low CO_2 emissions scenario simulations. For the intermediate emissions scenario, the occurrence probability of 2023-like events in the North China region by the end of this century will be 5.5 (range 4.9–6.3) times those under the 2023 climate, with an intensity 2.9 °C (range 2.4 °C–3.1 °C) higher than those under the 2023 climate. These findings highlight the need for adaptation measures to address the occurrence of 2023-like three-day heatwaves in North China in June even if carbon neutrality is achieved.

1. Introduction

The North China region emerged as a hotspot for heatwaves in June 2023. According to the National Climate Center of the China Meteorological Administration, 124 national meteorological stations in North China recorded temperatures >40 °C between 21 and 30 June 2023 (https://mp.weixin.qq.com/s/1sXlHt3xvLLixKGQel50_Q). The number of hot days, defined as a maximum temperature ⩾35 °C, in Beijing (15 d), Tianjin (13 d) and Shijiazhuang (18 d) in June was the highest in a single month in local observational history since 1961 (http://news.weather.com.cn/2023/06/3632314.shtml). Remarkably, the temperature at Beijing station (station ID 54511) was ⩾40 °C for three consecutive days during the dragon boat festival (an official public holiday with a large number of travelers) on 22–24 June 2023, which is unprecedented in the observational records for Beijing (http://news.weather.com.cn/2023/06/3630913.shtml).

This heatwave event was characterized by its strong intensity and extensive coverage, resulting in detrimental effects on transportation, public health, energy supply, agricultural development and economic growth. A car caught fire on the Badaling Expressway in Beijing on 22 June (https://m.gmw.cn/2023-06/29/content_1303422555.htm). The incidence of heatstroke increased compared with previous years, especially at some popular tourist sites (http://wjw.beijing.gov.cn/bmfw_20143/jkzs/jzjj/202306/t20230628_3148755.html), because the heatwave occurred during the three-day festival and the approaching summer travel season. The heatwave also led to a substantial increase in electricity demand, with the maximum load in Hebei Province's power grid reaching a peak from the beginning of summer 2023 to 24 June, increasing by 4.83% compared with the same period in 2022 (www.sohu.com/a/690591135_121123888). The power grid load in Beijing increased by 30% compared with the same period in 2022, with cooling demand accounting for 35% of the total load (https://news.bjd.com.cn/2023/06/23/10473651.shtml). Central and northern Hebei Province experienced a moderate to severe meteorological drought, resulting in the accelerated depletion of soil moisture and the delayed emergence of summer crops such as corn (www.cma.gov.cn/wmhd/2011wzbft/2011wzxzb/xwfbh_2307/index.html).

It remains unclear how much of these exceptional heatwave events can be related to anthropogenic climate change. It is also unclear how frequent and intense such strong heatwave events will be in the future. These questions fall into the realm of event attribution, which seeks to quantitatively answer whether, and to what extent, anthropogenic climate change has altered the characteristics—predominantly the probability and intensity—of particular events [1–4]. Event attribution analyses of heatwave events in China have been carried out in several previous studies (e.g. [5–10]). However, these attribution analyses were carried out months or even years after the event when both the media and the public had lost interest.

We carried out a rapid attribution analysis of this extreme heatwave event to answer these questions. A rapid attribution study can respond timely to issues of concern to the general public and inform them how climate change is linked to the severe weather they have recently experienced. This will increase their awareness and may lead to participation in climate action to reduce the effects of climate change on human society. It can also provide risk information on climate change and thus inform policy-making for climate change adaptation [11]. Europe [12], the USA [13], New Zealand [14] and South Africa [15] have been developing their own practical real-time attribution services. This study will benefit the establishment of real-time attribution services in China. We used two probability-based attribution approaches—an empirical approach based on observations and a coupled model approach based on phase 6 of the coupled model intercomparison project (CMIP6) model simulations—to make attribution assessments as also used in the world weather attribution (WWA) Protocol [16]. However, in contrast with the WWA Protocol, we used a different strategy in the CMIP6 model attribution and future projections. In addition, we included a very low emissions scenario in which carbon neutrality is achieved (shared socioeconomic pathway 1–1.9 (SSP1-1.9) [17]) in the future projections to show the situation in this optimistic scenario and to discuss measures to adapt to heatwaves. This scenario has only recently become available in the CMIP6 models and has seldom been used in previous attribution studies.

2. Data and methods

2.1. Data

We used the European center for medium-range weather forecasts (ECMWF) ERA5 reanalysis dataset [18] to represent the observations because station observations in China are not released quickly enough for a rapid attribution study. The immediacy of the ERA5 dataset makes it suitable for rapid attribution research. Because daily data products are not provided directly in the ERA5 dataset, we selected the gridded hourly 2 m temperature (surface-level products) and geopotential height (GPH; pressure-level products) data with a spatial resolution of 1.0° from the ERA5 hourly reanalysis dataset for the time period 1959–2023. We derived the daily maximum temperature (T_{max}) using the daily maximum of the hourly 2 m temperature data as instructed by the ECMWF and derived the daily GPH at 500 hPa from the average of the 24 h data. We also used the daily average volumetric soil water of the top layer (swvl1), which ranges from 0 to 7 cm beneath the surface, to analyze the soil moisture content.

The model simulations were from the daily products of CMIP6 multi-model ensembles [19]. Four experiments were used, including an historical simulation with anthropogenic forcing and natural factors combined (historical), the SSP2-4.5 scenario simulations [17], the SSP1-1.9 scenario simulations [17] and natural forcing only (hist-nat) simulations. The SSP2-4.5 scenario is an intermediate greenhouse

Table 1. CMIP6 models, simulation experiments, number of ensemble members for each experiment and model evaluation results based on the Kolmogorov–Smirnoff test. An asterisk (*) indicates that the model passed the test and was included in the attribution analyses.

Model	Historical	SSP2-4.5	SSP1-1.9	Hist-nat	p
ACCESS-CM2	10	5	/	3	0.460*
ACCESS-ESM1-5	40	40	/	3	0.324*
CanESM5	50	50	50	10	0.717*
FGOALS-g3	5	3	/	3	0.836*
HadGEM3-GC31-LL	5	5	/	10	0.255*
IPSL-CM6A-LR	33	11	6	6	0.506*
MIROC6	50	50	50	50	0.170*
MRI-ESM2-0	12	5	5	5	0.394*
NorESM2-LM	3	3	/	3	0.722*

gas emissions scenario, generally representing the situation of the past evolution, whereas the SSP1-1.9 scenario is a carbon neutrality scenario with CO_2 emissions decreasing to net zero around 2060 followed by net-negative CO_2 emissions [20]. The SSP1-1.9 scenario is used to explore the situation in a very low CO_2 emissions scenario to inform adaptation measures. Table 1 lists the detailed model names and numbers of the ensembles. We used the SSP2-4.5 simulations to connect the historical simulations and extend the data to 2023 (historical-SSP2-4.5).

2.2. Methods

2.2.1. Event definition

Beijing experienced three consecutive days with temperatures ⩾40 °C from 22 to 24 June 2023, which is very unusual in the observational history. We therefore defined this event as the maximum three-day average T_{max} in June. We then calculated the area-weighted average over the North China region (113.5–120° E, 34.5–42.5° N) to obtain an index (Tx3d). We estimated its linear trend and statistical significance using the iteration-based non-parametric method described in Wang and Swail [21] and took into account repeated values in the time series [22].

2.2.2. Event attribution approaches

The general approach in the rapid attribution of extreme events is a classical probability-based approach [16]. We used two probability-based attribution approaches [1, 3, 4] for making attribution assessments: an empirical approach [2, 4, 23] based on observations and a coupled model approach [1, 2, 4] based on the CMIP6 model simulations. This multi-method, multi-model attribution was also adopted in the WWA Protocol [16]; however, we used a different strategy from the WWA in the CMIP6 model attribution and future projection as described in detail in the following.

For the empirical approach, we used the generalized extreme value (GEV) shift-fit method adopted in the WWA Protocol and described by van Oldenborgh *et al* [23], Philip *et al* [16] and van Oldenborgh *et al* [11]. We assumed that the trend of Tx3d shifts with the four-year smoothed global mean surface temperature (GMST) anomaly and that the location parameter μ of the GEV distribution is linearly correlated with the smoothed GMST—that is, $\mu_t = \mu_0 + a\text{GMST}_t$. This assumption is commonly used for temperature events and has been found to hold well in studies using large ensembles of model simulations with sufficient data for analysis without relying on statistical fitting [16, 24, 25]. The non-stationary GEV distribution was fitted to Tx3d based on the ERA5 dataset with the 2023 value to obtain the parameters. We then used the smoothed GMST values of any year to obtain the GEV distribution under that year's climate. We compared the occurrence probability of Tx3d exceeding the intensity of the 2023 event under the present climate (GMST_{2023}) (P_1) and under the pre-industrial climate ($\text{GMST}_{-1.2}$, −1.2 °C cooler than the climate in 2023, www.globalwarmingindex.org) (P_0). The latter represents the absence of anthropogenic climate change effects. We calculated the probability ratio ($\text{PR} = P_1/P_0$; [26]) and the fraction of attributable risk ($\text{FAR} = 1 - P_0/P_1$; [1]) to quantify the influence of anthropogenic climate change on the frequency change of 2023-like events. The PR is the factor by which the occurrence probability of similar events has changed and the FAR indicates the proportion of the risk of such events being attributable to anthropogenic climate change. We also calculated the intensity change of similar events (e.g. [27]) with the same return period as the 2023 event under the two climate conditions. The uncertainty ranges of the PR, FAR and intensity change were calculated using bootstrap resampling (1000 times).

For the coupled model approach, we used a time slice of 21 years (2013–2033) centered on the year of the event (2023) in the historical-SSP2-4.5 simulations to represent the climate state of 2023 with anthropogenic forcings (historical_{2023}). We used all the available hist-nat simulation data from 1850 to 2020 to represent the climate state of 2023 without anthropogenic forcings (hist-nat_{2023})

because the hist-nat simulations during this era are almost stationary. This method is similar to that used by Christidis and Stott [28]. Because the model simulations have different resolutions, we interpolated them into the same (1° × 1°) resolution as the ERA5 dataset. To avoid the model biases in the mean value of Tx3d, we removed the ensemble mean of the historical simulation averaged over the climatological period (1961–1990) from each experiment for each model and then replaced it with the observed climatological mean. After this correction, we checked the distributions from 1959 to 2014 between the observations and the bias-corrected historical simulations using the Kolmogorov–Smirnoff test. Only the models that passed the evaluation were included in the subsequent attribution analysis. As in the empirical approach, we also calculated PR, FAR and the change in intensity to represent the effect of anthropogenic climate change under the $historical_{2023}$ climate relative to the $hist\text{-}nat_{2023}$ climate.

To investigate possible future changes in the North China region, we calculated PR and the change in intensity using SSP2-4.5/SSP1-1.9 scenario simulations of three typical future time slices and compared these with the 2023 climate ($historical_{2023}$) to represent any additional change. One time slice is the year 2035 (using 2025–2045 to represent the 2035 climate) to relate to the National Climate Change Adaptation Strategy 2035 in China. This strategy focused on overall guidance, communication, coordination, strengthening observations and the assessment of climate change impacts to improve the ability of major sectors and key vulnerable regions to adapt to climate change. The second and third time slices are the mid-century (using 2040–2060 to represent the 2050 climate) and the end of century (using 2080–2100 to represent the 2090 climate).

3. Results

3.1. Characteristics of the event

The absolute T_{max} in the North China region was exceptionally high from 22 to 24 June 2023, with most areas in the study region exceeding 35 °C (figure 1(a)). T_{max} is generally higher in the North China region than in other areas of China, except for the desert area of Xinjiang Uygur Autonomous Region in northwestern China (figure 1(a)). The temperature anomaly in North China is also very high, with a value of about 2.9 °C–9.4 °C (figure 1(b)). Tx3d in North China from 22 to 24 June 2023 was the highest three-day average T_{max} in June since 1959 (figure 1(c)). The intensity of the 2023 event was 3.4 standard deviations. The linear trend in Tx3d in North China region in June for the time period 1959–2023 shows an increasing tendency at a rate of +0.13 °C/decade (95% confidence interval −0.12 to 0.40 °C/decade), although this is not statistically significant. This implies that both the internal variability and climate change had a role in the intensity of the 2023 heatwave event.

3.2. Background circulations

An important factor in causing an extreme event is the anomalous atmospheric circulation. To provide context for the subsequent event attribution study, we conducted a brief analysis of the direct factors responsible for the heatwave, focusing on the GPH at 500 hPa. We calculated the linearly detrended GPH anomaly because GPH is influenced by lower tropospheric temperatures, which are rising with human-induced climate change. It is clear that a strong continental high-pressure ridge system dominated the whole of North China and its adjacent regions from 22 to 24 June 2023 (figure 2(a)). This anomalous warm core high-pressure system and the associated strong sinking flow (figure 2(b)) enhanced insolation and adiabatic heating in North China. The high-pressure system began to influence the study region on 21 June and then receded after 25 June (figure S1) and was therefore the major system inducing the heatwave in this region. It is worth noting that the soils were anomalously dry in both the week preceding and during the heatwave event (figures 2(c) and (d)), which exacerbated the intensity of the heatwave.

3.3. Event attribution

The empirical approach showed that the mean GEV distribution for the Tx3d increased with a smoothed GMST at a rate of +1.03 °C/°C (figure S2(a)). The return period at the 2023 climate state is about 111 years (95% uncertainty margin of 24.3 years to +∞) (figure S2(b)), which means that an extreme heatwave in June as observed in 2023 has a probability of about 0.9% each year at the 2023 climate state, with a 95% uncertainty margin of 0%–4.1%. It is therefore a low-likelihood, high-impact event. The comparison of the fit for the 2023 climate and for a pre-industrial climate (figure 3(a)) shows a PR of about 58 (range 0.6 to +∞, statistically not significant) (figure 3(c), table 2), corresponding to an FAR of about 0.98 (range −0.74 to 1) (figure 3(c), table 2) and an increase in intensity of Tx3d of about 1.2 °C (range 0.01 °C–2.5 °C, statistically significant) (figure 3(d), table 2).

In the coupled model approach, all the models used passed the model evaluation (table 1), with p reaching 0.53 when pooling all model ensembles (figure S3). All nine models were therefore included in the attribution analysis. As in the empirical

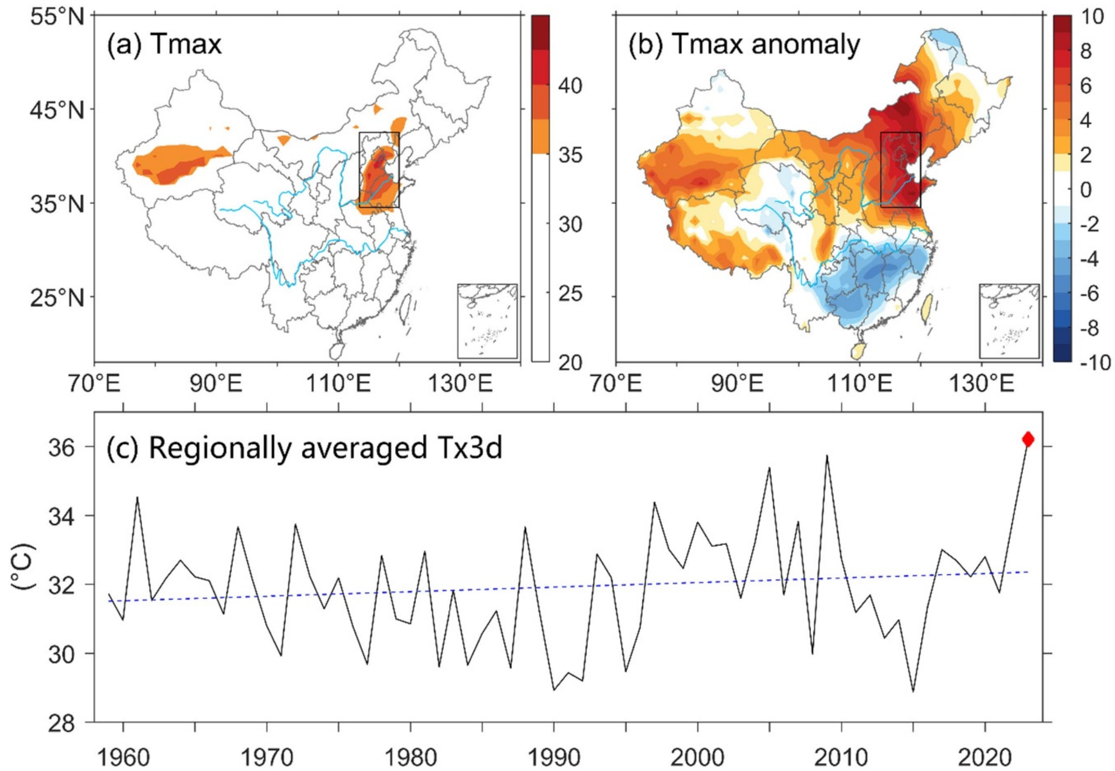

Figure 1. Characteristics of the heatwave event in North China from 22 to 24 June 2023. (a) T_{max} averaged over the three days; only values $\geqslant$35 °C are shown. The rectangle indicates the study region. (b) Anomaly of T_{max} relative to the 1961–1990 base period. (c) Highest three-day average T_{max} (Tx3d) in the study region in June for the time period 1959–2023. The red dot is 2023. The blue dashed line indicates the linear trend.

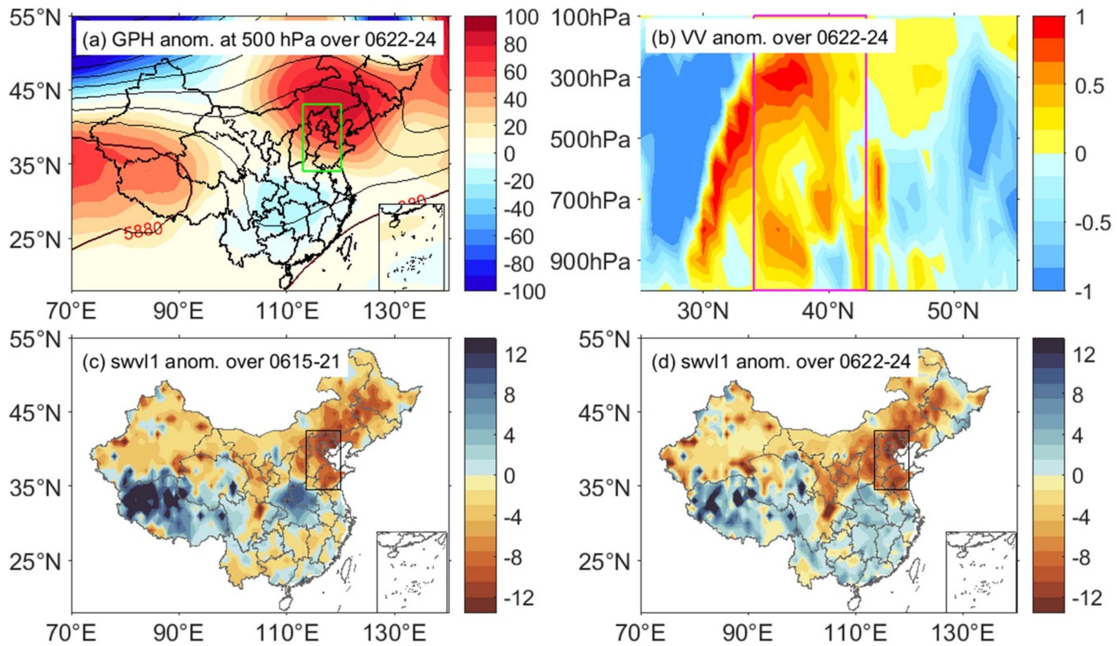

Figure 2. (a) Spatial pattern of the geopotential height (GPH) (contours; units: gpm) and detrended GPH anomaly (shading; units: gpm) at 500 hPa from 22 to 24 June 2023; the rectangle indicates the study area. (b) Zonally averaged vertical velocity (VV) anomaly (shading; units: 0.1 Pa $\cdot$ s^{-1}) from the land surface to 100 hPa. Negative values indicate upward motion. (c) Spatial pattern of the volumetric soil water content of the top soil layer (swvl1) anomaly (shading; units: 10^{-2} m^3 $\cdot$ m^{-3}) from (c) 15–21 June 2023 and (d) from 22 to 24 June 2023; the rectangle indicates the study area. Negative values indicate drier soils. The anomalies are calculated relative to the 1961–1990 base period.

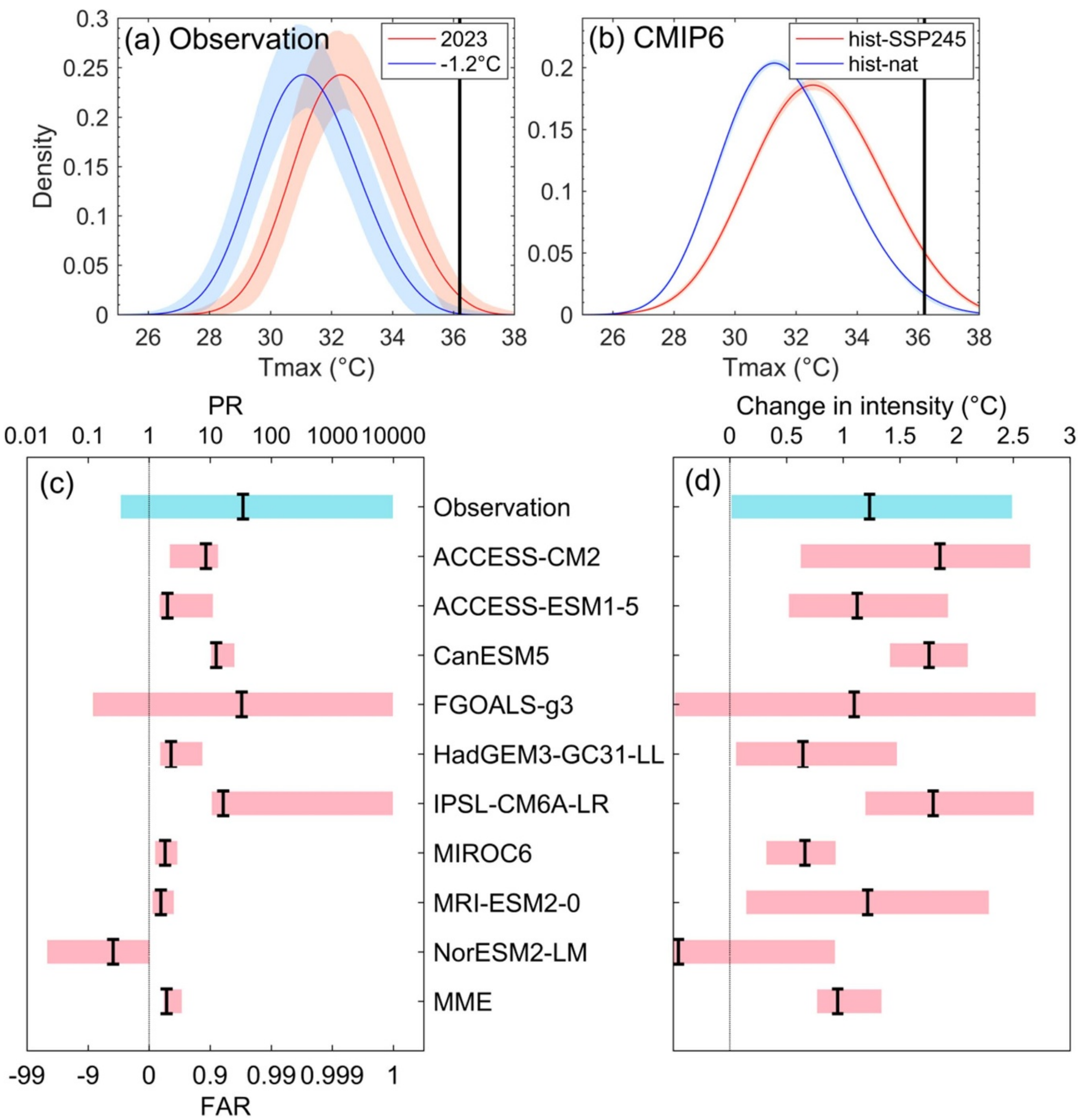

Figure 3. Attribution analyses of the heatwave event in North China from 22 to 24 June 2023. (a) Generalized extreme value (GEV) distributions fitted to the 2023 climate in the ERA5 dataset (red) and to the pre-industrial climate (blue). The vertical solid line indicates the threshold (the intensity of the heatwave event in 2023). Shaded areas indicate the 2.5%–97.5% uncertainty range. (b) GEV distributions fitted to the 2023-like events in the hist-SSP2-4.5 simulations (red) and hist-nat simulations (blue) from the CMIP6 models. (c) Probability ratio (PR) and corresponding fraction of attributable risk (FAR) for 2023-like heatwave events under a near-present-day climate compared with those under a counterfactual climate without human influences. (d) Change in intensity for 2023-like heatwave events under a near-present-day climate compared with those under a counterfactual climate without human influences. MME indicates the results from pooling all multi-model ensembles.

Table 2. Probability ratio and change in intensity when comparing two climate conditions. The first row compares the climate of $GMST_{2023}$ with $GMST_{-1.2}$. The second row compares $historical_{2023}$ with $hist\text{-}nat_{2023}$. The remaining rows compare the climate shown in the first column with the 2023 climate. 95% confidence intervals are shown in the parenthesis. An asterisk (*) indicates the result was statistically significant.

Dataset	Probability ratio	Intensity
Observations	58.4 (0.57, $+\infty$)	1.2 (0.01, 2.49)*
Hist-SSP2-4.5	3.6 (3.09, 5.89)*	1.0 (0.77, 1.34)*
2035 climate in SSP2-4.5	1.6 (1.39, 1.87)*	0.5 (0.31, 0.75)*
2050 climate in SSP2-4.5	2.7 (2.35, 3.13)*	1.4 (0.88, 1.62)*
2090 climate in SSP2-4.5	5.5 (4.90, 6.26)*	2.9 (2.44, 3.12)*
2035 climate in SSP1-1.9	2.0 (1.57, 2.58)*	0.8 (0.40, 1.17)*
2050 climate in SSP1-1.9	2.2 (1.87, 2.91)*	0.8 (0.53, 1.18)*
2090 climate in SSP1-1.9	1.6 (1.27, 2.05)*	0.5 (0.19, 0.84)*

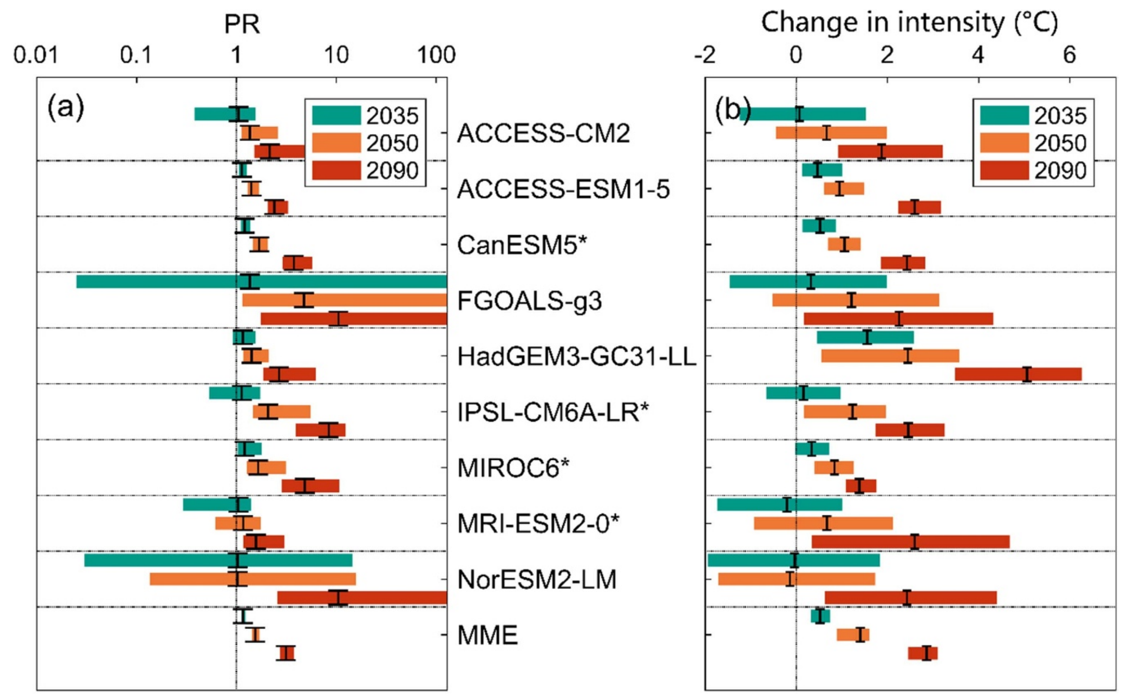

Figure 4. Projection results of the 2023-like heatwave events in North China based on the SSP2-4.5 simulations. (a) Probability ratio (PR) for 2023-like heatwave events under typical future climate conditions compared to those under the 2023 climate. (b) Change in intensity for 2023-like heatwave events under typical future climate conditions compared to those under the 2023 climate. MME indicates the results from pooling all multi-model ensembles.

approach (figure 3(a)), the probability distribution curve shifted toward warmer temperatures when anthropogenic climate change was included (figure 3(b)). The comparison of the fit for the $historical_{2023}$ and $hist\text{-}nat_{2023}$ simulations using the pooled CMIP6 model ensembles (figure 3(b)) showed a PR of about 3.6 (range 3.1–5.9, statistically significant) (figure 3(c), table 2), corresponding to an FAR of about 0.72 (range 0.68–0.83) (figure 3(c), table 2) and an increase in intensity of Tx3d of about 1.0 °C (range 0.8 °C–1.3 °C, statistically significant) (figure 3(d), table 2). Although the statistical significance varied among individual models, seven of the nine models showed a consistent statistically significant PR (figure 3(c)) and a change in intensity (figure 3(d)), although the FGOALS-g3 and NorESM3-LM models were not statistically significant (figures 3(c) and (d)).

3.4. Future projections

The questions that naturally follow are how likely will the 2023-like Tx3d be in the future and will it be the new normal? we used the coupled model approach to calculate the PR and change in the intensity by comparing the 2035 climate, the 2050 climate and the 2090 climate with the 2023 climate based on the SSP2-4.5 simulations. The results show a PR of about 1.6 (range 1.4–1.9), 2.7 (range 2.4–3.1) and 5.5 (range 4.9–6.3), respectively, for the three future climate conditions based on the pooling of the CMIP6 models (figure 4(a), table 2). Accordingly, the change in intensity is about 0.5 °C (range 0.3 °C–0.8 °C), 1.4 °C (range 0.9 °C–1.6 °C) and 2.9 °C (range 2.4 °C–3.1 °C), respectively (figure 4(b), table 2). These values are all statistically significant and indicate that the occurrence probability of 40 °C in June in the North China region will become more likely in the future and the intensity of 2023-like three-day heatwave events will become more intense. All nine models show consistent statistically significant results for the North China region at the end of the century (figures 4(a) and (b)).

When we used the SSP1-1.9 simulations to calculate the PR and the change in intensity, the increase in magnitude was smaller in the middle of the century and at the end of the century compared with those using the SSP2-4.5 simulations, especially for the end of the century (figure 5, table 2). This indicates the benefits of carbon neutrality. However, the increase will still be statistically significant, with a PR of about 1.6 (range 1.3–2.1) and an intensity of an additional 0.5 °C (range 0.2 °C–0.8 °C) at the end of the century versus the 2023 climate (figure 5, table 2). This means that we still need to adapt to 2023-like three-day heatwave events in June for the rest of this century and that these events will also occur more often and be more intense than in 2023 even if carbon neutrality is achieved.

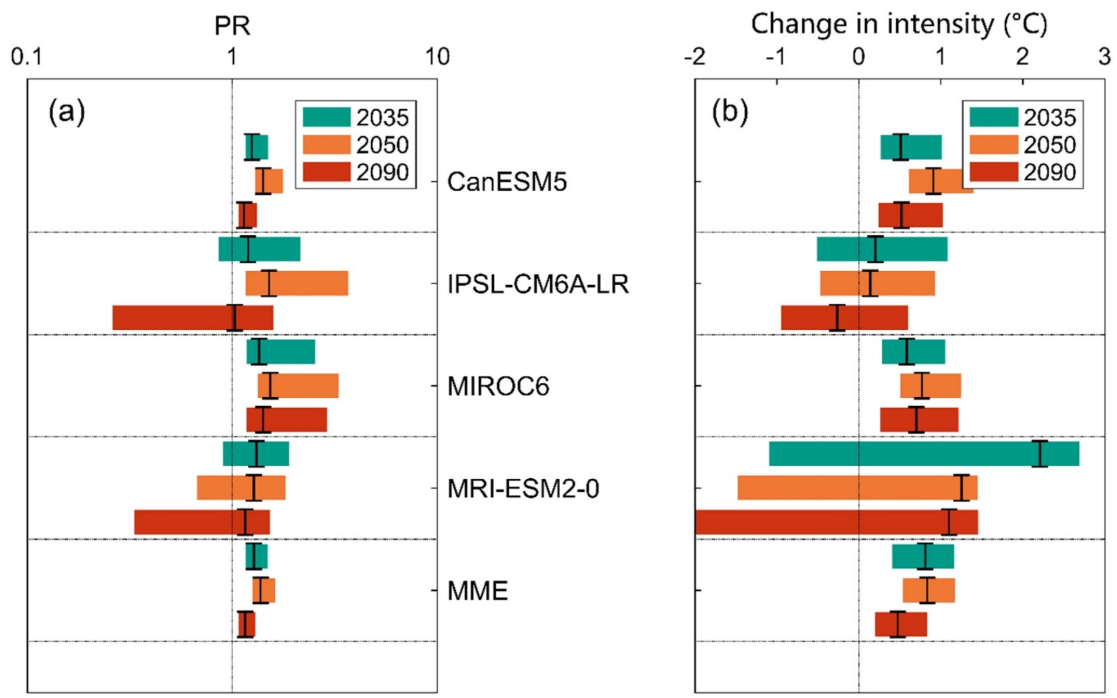

Figure 5. As in figure 4, but based on the SSP1-1.9 simulations.

4. Conclusions and discussions

The record-breaking heatwave event in the North China region from 22 to 24 June 2023 occurred under the background of an anomalous high-pressure system controlling the region during this period and was amplified by anomalously dry soils before and during the heatwave event. Attribution analyses from both the empirical approach based on observations and the coupled model approach based on the CMIP6 model simulations consistently showed that the intensity of 2023-like Tx3d events has been significantly increased by at least 1.0 °C (range 0.8 °C–1.3 °C) due to anthropogenic climate change. Future projections indicate that 2023-like Tx3d events in North China in June will occur at least 1.6 (range 1.3–2.1, statistically significant) times during the rest of this century and will be at least 0.5 °C (range 0.2 °C–0.8 °C, statistically significant) more intense than events under the 2023 climate even if carbon neutrality is achieved based on the very low CO_2 emissions scenario (SSP1-1.9). If we use the intermediate emissions scenario (SSP2-4.5), then the occurrence probability of 2023-like Tx3d events in North China at the end of this century will be 5.5 (range 4.9–6.3) times and the intensity will be 2.9 °C (range 2.4 °C–3.1 °C) stronger than events under the 2023 climate.

It should be noted that if we did not use the 2023 value to fit the GEV shift model, then the return period under the 2023 climate state would be about 336 years (95% uncertainty margin of 49.5 to $+\infty$) (figure not shown, but similar to figure S2(b)), the occurrence probability of which would be much rarer than (only one-third of) that reported here. Our return period can therefore be considered to be a conservative estimate.

Extreme three-day heatwave events in North China in June are projected to occur more often and be more intense in the future than under the present climate. The greatest threat to humans from heatwaves is their impact on our health. The two most effective ways of adapting to extreme heat are managing the health risks and reducing exposure to heat. Countries need to adopt a range of effective interventions to manage public health risks, including the development of comprehensive heat adaptation plans by government departments and the establishment of timely and effective early warning systems for heat-health to facilitate monitoring and give early warnings of heat-related risks. Communities should also provide education about the effects of extreme heat and communicate the risks to help residents better protect themselves from such extreme events. Reducing heat exposure, especially for vulnerable populations, is also an important protective measure. Cities can reduce the urban heat island effect by planning the spatial distribution of buildings, optimizing building design and greening urban areas. Individuals can reduce the effects of heat exposure by staying hydrated and avoiding outdoor activities during periods of peak heat.

Data availability statement

The ERA5 data are publicly available at www.ecmwf.int/en/forecasts/dataset/ecmwf-reanalysis-v5. The CMIP6 data are publicly available at https://esgf–node.llnl.gov/projects/cmip6/.

Acknowledgments

This study was sponsored by the National Natural Science Foundation of China (Grant No. 42341203), the Chinese Academy of Sciences Project for Young Scientists in Basic Research (Grant No. YSBR-086) and the Jiangsu Collaborative Innovation Center for Climate Change. The authors thank the two anonymous reviewers for their comments and suggestions, which helped to improve this paper.

ORCID iD

Cheng Qian https://orcid.org/0000-0001-6158-9494

References

[1] Stott P A, Stone D A and Allen M R 2004 Human contribution to the European heatwave of 2003 *Nature* **432** 610–4

[2] Stott P A *et al* 2016 Attribution of extreme weather and climate-related events *WIRES Clim. Change* **7** 23–41

[3] Seneviratne S I *et al* 2021 *Climate Change 2021: The Physical Science Basis* (Cambridge University Press)

[4] Qian C, Ye Y B, Chen Y and Zhai P M 2022 An updated review of event attribution approaches *J. Meteorol. Res.* **36** 227–38

[5] Sun Y, Zhang X B, Zwiers F W, Song L C, Wan H, Hu T, Yin H and Ren G Y 2014 Rapid increase in the risk to extreme summer heat in eastern China *Nat. Clim. Change* **4** 1082–5

[6] Miao C, Sun Q, Kong D and Duan Q 2016 Record-breaking heat in Northwest China in July 2015: analysis of the severity and underlying causes *Bull. Am. Meteorol. Soc.* **97** S97–S101

[7] Ma S, Zhou T, Stone D A, Angelil O and Shiogama H 2017 Attribution of the July-August 2013 heat event in central and eastern China to anthropogenic greenhouse gas emissions *Environ. Res. Lett.* **12** 054020

[8] Chen Y, Chen W, Su Q, Luo F, Sparrow S, Wallom D, Tian F, Dong S F B, Tett S F B and Lott F C 2019 Anthropogenic warming has substantially increased the likelihood of July 2017-like heat waves over central eastern China *Bull. Am. Meteorol. Soc.* **100** S91–S95

[9] Zhou C, Wang K, Qi D and Tan J 2019 Attribution of a record-breaking heatwave event in summer 2017 over the Yangtze River delta *Bull. Am. Meteorol. Soc.* **100** S97–S103

[10] Ye Y and Qian C 2021 Conditional attribution of climate change and atmospheric circulation contributing to the record-breaking precipitation and temperature event of summer 2020 in southern China *Environ. Res. Lett.* **16** 044058

[11] van Oldenborgh G J *et al* 2021 Pathways and pitfalls in extreme event attribution *Clim. Change* **166** 13

[12] Otto F E L, Kew S, Philip S, Stott P and Van Oldenborgh G J 2022 How to provide useful attribution statements: lessons learned from operationalizing event attribution in Europe *Bull. Am. Meteorol. Soc.* **103** S21–S25

[13] Barsugli J J *et al* 2022 Development of a rapid response capability to evaluate causes of extreme temperature and drought events in the United States *Bull. Am. Meteorol. Soc.* **103** S14–S20

[14] Tradowsky J S, Bird L, Kreft P V, Rosier S M, Soltanzadeh I, Stone D A and Bodeker G E 2022 Toward near-real-time attribution of extreme weather events in Aotearoa New Zealand *Bull. Am. Meteorol. Soc.* **103** S105–10

[15] Stone D A, Lawal K A, Lennard C, Tadross M, Wolski P and Wehner M F 2022 The life and times of the weather risk attribution forecast *Bull. Am. Meteorol. Soc.* **103** S1–S6

[16] Philip S *et al* 2020 A protocol for probabilistic extreme event attribution analyses *Adv. Stat. Climatol. Meteorol. Oceanogr.* **6** 177–203

[17] O'Neill B C *et al* 2016 The scenario model intercomparison project (scenariomip) for CMIP6 *Geosci. Model Dev.* **9** 3461–82

[18] Hersbach H *et al* 2020 The ERA5 global reanalysis *Q. J. R. Meteorol. Soc.* **146** 1999–2049

[19] Eyring V, Bony S, Meehl G A, Senior C A, Stevens B, Stouffer R J and Taylor K E 2016 Overview of the coupled model intercomparison project phase 6 (CMIP6) experimental design and organization *Geosci. Model Dev.* **9** 1937–58

[20] Riahi K *et al* 2017 The shared socioeconomic pathways and their energy, land use, and greenhouse gas emissions implications: an overview *Glob. Environ. Change* **42** 153–68

[21] Wang X L and Swail V R 2001 Changes of extreme wave heights in Northern Hemisphere oceans and related atmospheric circulation regimes *J. Clim.* **14** 2204–21

[22] Qian C, Zhang X B and Li Z 2019 Linear trends in temperature extremes in China, with an emphasis on non-Gaussian and serially dependent characteristics *Clim. Dyn.* **53** 533–50

[23] Van Oldenborgh G J, Haarsma R, De Vries H and Allen M R 2015 Cold extremes in North America vs. Mild weather in Europe the winter of 2013–14 in the context of a warming world *Bull. Am. Meteorol. Soc.* **96** 707–14

[24] Kew S F, Philip S Y, Jan van Oldenborgh G, van der Schrier G, Otto F E L and Vautard R 2019 The exceptional summer heat wave in southern Europe 2017 *Bull. Am. Meteorol. Soc.* **100** S49–S53

[25] Sippel S, Otto F E L, Flach M and van Oldenborgh G J 2016 The role of anthropogenic warming in 2015 central European heat waves *Bull. Am. Meteorol. Soc.* **97** S51–S56

[26] Fischer E M and Knutti R 2015 Anthropogenic contribution to global occurrence of heavy-precipitation and high-temperature extremes *Nat. Clim. Change* **5** 560–4

[27] Otto F E L, Massey N, van Oldenborgh G J, Jones R G and Allen M R 2012 Reconciling two approaches to attribution of the 2010 Russian heat wave *Geophys. Res. Lett.* **39** L04702

[28] Christidis N and Stott P A 2022 Anthropogenic climate change and the record-high temperature of May 2020 in western Europe *Bull. Am. Meteorol. Soc.* **103** S33–S37